Inorg. Chem. **2004**, *43*, 5537–5542

Inorganic Chemistry Article

Synthesis and Characterization of ReO_4-Containing Microporous and Open Framework Structures

Junhua Luo,[†] Ben Alexander,[‡] Timothy R. Wagner,[‡] and Paul A. Maggard*[,†]

Department of Chemistry, North Carolina State University, 2620 Yarbrough Drive, Raleigh, North Carolina 27695-8204, and Department of Chemistry, Youngstown State University, 1 University Plaza, Youngstown, Ohio 44555

Received March 23, 2004

A microporous and an open framework structure, $[Cu_2(pzc)_2(H_2O)_2ReO_4]$ (**I**) and $[Cu(pzc)(H_2O)ReO_4]\cdot 2H_2O$ (**II**) (pzc = 2-pyrazinecarboxylate), respectively, have been prepared using hydrothermal methods and characterized using IR, TGA, and X-ray diffraction (**I** *Pnma*, No. 62, $Z = 4$, $a = 7.4949(9)$ Å, $b = 24.975(3)$ Å, $c = 9.141(1)$ Å; **II** $P2_1/c$, No. 14, $Z = 4$, $a = 8.5878(9)$ Å, $b = 12.920(1)$ Å, $c = 9.741(1)$ Å, $\beta = 92.830(2)°$). **I** and **II** crystallize as red and blue solids, respectively, and each contains chains constructed from alternating $Cu(pzc)_2/ReO_4$ oxide-bridged metal sites. The bidentate pzc ligand further bridges each –Cu–O–Re–O– chain to adjacent chains, via the Cu sites, to form a 3D net in **I**, with ellipsoidal channels that are ~3.3–4.7 Å × 12.5 Å, and in **II**, stacked layers of square nets with H_2O-filled cavities that are ~4.4 × 5.1 Å. Local ReO_4^- groups, a component of common oxidation catalysts, are directed at the channels and cavities of each structure, respectively. Thermogravimetric analysis indicates that **I** loses up to 64% of its H_2O content before decomposition at 225 °C, while **II** loses ~100% of its H_2O content by 265 °C.

Introduction

In the past several years, synthetic engineering of open-framework inorganic/organic materials has been highlighted as a means by which chemists can uncover and target new solid structures and properties through selection of the appropriate solid-state building blocks.[1−6] While the organic component is envisioned to assist in the formation of the desired structural topology, the inorganic component is often cited for its potential to impart a particular physical property. Recent examples include numerous types of metal−organic vanadates,[3] molybdates,[4] and phosphates,[5] which exist in a variety of open framework forms that make them potentially useful as catalysts, as cathode battery materials, and for ion absorption/exchange, among others.

Remarkably absent from the list of known open-framework solids to date has been the synthesis of analogous metal−organic rhenate (e.g., ReO_4^-) compounds. By themselves, simple rhenium oxides exhibit multiple oxygen coordination environments and several (high) rhenium oxidation states. For example, Re(VII) centers distorted oxide tetrahedra and octahedra that link via vertexes in Re_2O_7,[7] while in ReO_3 and in the two reported structure types for ReO_2,[8,9] corner-sharing octahedra are centered by Re(VI) and Re(IV), respectively. Owing to the rich redox chemistry, and the associated coordination environments for rhenium, rhenium oxides are increasingly used as (selective oxidation) catalysts. Examples include oxorhenium complexes in solution,[10] Re_2O_7/Al_2O_3 (including on $/TiO_2$, $/ZrO_2$, $/SiO_2$, and /MgO) supported catalysts,[11−13] tetrahedral oxorhenium species

* Author to whom correspondence should be addressed. E-mail: Paul_Maggard@ncsu.edu.

[†] North Carolina State University.

[‡] Youngstown State University.

(1) Cheetham, A. K.; Ferey, G.; Loiseau, T. *Angew. Chem., Int. Ed.* **1999**, *38*, 3268−3292.

(2) Rao, C. N. R.; Natarajan, S.; Vaidhyanathan, R. *Angew. Chem., Int. Ed.* **2004**, *43* (12), 1466.

(3) Hagrman, P. J.; Finn, R. C.; Zubieta, J. *Solid State Sci.* **2001**, *3*, 745−774.

(4) Hagrman, P. J.; Hagrman, D.; Zubieta, J. *Angew. Chem., Int. Ed.* **1999**, *38*, 2638.

(5) Lii, K.-W.; Huang, Y.-F.; Zima, V.; Huang, C.-Y.; Lin, H.-M.; Jiang, Y.-C.; Liao, F.-L.; Wang, S.-L. *Chem. Mater.* **1998**, *10*, 2599.

(6) Feng, S.; Xu, R. *Acc. Chem. Res.* **2001**, *34*, 239−247.

(7) (a) Krebs, B.; Müller, A.; Beyer, H. H. *Inorg. Chem.* **1969**, *8*, 436. (b) Krebs, B.; Müller, A.; Beyer, H. *Chem. Commun.* **1968**, *43*, 263−264.

(8) (a) Meisel, K. *Z. Anorg. Allg. Chem.* **1932**, *207*, 121. (b) Blitz, W. *Z. Anorg. Allg. Chem.* **1933**, *214*, 225−238.

(9) (a) Magneli, A. *Acta Chem. Scand.* **1957**, *11*, 28. (b) Rogers, D. R.; Shannon, R. D.; Sleigh, A. W.; Gillson, J. L. *Inorg. Chem.* **1969**, *8*, 841−849.

(10) Huang, R.; Espenson, J. H. *J. Mol. Catal. A* **2001**, *168*, 39.

10.1021/ic049609h CCC: $27.50

Published on Web 08/13/2004

incorporated into HZSM-5[14] and supported on α,γ-Fe_2O_3 and V_2O_5,[15] and deposition of ReO_4^- (and subsequent reduction to ReO_2) onto metals such as Ni, Pd, Co, and Cu,[16−19] to mention a few. However, in the area of mixed inorganic/organic solids, relatively very few examples are known to contain rhenium oxide as one of the potential "active" components within an open metal−organic framework. The list of related metal−organic/ReO_4 solids currently includes ~7 simple metal salts with either urea or thiourea as the organic component,[20−24] the molecular $M(py)_4(ReO_4)_2$ (M = Zn, Cd) trimers,[25,26] the molecular phthalocyanines (= pc) $Cu(pc)(ReO_4)_2$,[27] $[Ni(pc)]_3[ReO_4]_2$·(npCl) (npCl = chloronaphthalene),[28] and $[Ag_4(2,2'\text{-bpy})_4[ReO_4]_2\cdot(ReO_4)_2$.[29] In these examples, ReO_4 tetrahedra exhibit both terminal and bridging bonding modes (sometimes both within the same structure) and therefore could form the basis for constructing a large variety of open network types that arise from corner-sharing tetrahedra, as is common for zeolitic solids.

Our research efforts to access solid state structures with potentially catalytically active sites led us to synthetically explore the ReO_x/Cu−organic systems for the occurrence of new porous and layered structures. Using 2-pyrazinecarboxylate (pzc) as the organic component, we report herein the synthesis and characterization of new and relatively uncommon ReO_4-containing microporous and open framework structures, featuring some of the first such examples with Re to have a 3D network with channels, $[Cu_2(pzc)_2(H_2O)_2ReO_4]$ (**I**), and also another with a hydrated layered structure $[Cu(pzc)(H_2O)ReO_4]\cdot 2H_2O$ **(II)**, that are close in structure and composition.

Experimental Section

Materials and Methods. Re_2O_7 (99.99+%), Cu_2O (99.99%+), and 2-pyrazinecarboxylic acid (99+%) were obtained from Alfa Aesar and used as received. Reagent amounts of deionized water were also used in the syntheses. FEP Teflon pouches were shaped by cutting the film into squares, folding the squares in half, and sealing two of the edges to make a 3-in. × 2-in. container.

Preparation of $[Cu_2(pzc)_2(H_2O)_2ReO_4]$ (I) and $[Cu(pzc)(H_2O)ReO_4]\cdot 2H_2O$ (II). For both solids the hydrothermal synthesis was performed by adding 2.93×10^{-1} g (6.05×10^{-4} mol) of Re_2O_7, 8.66×10^{-2} g (6.05×10^{-4} mol) of Cu_2O, 7.51×10^{-2} g (6.05×10^{-4} mol) of 2-pyrazinecarboxylic acid, and 5.45×10^{-1} g (3.03×10^{-2} mol) of H_2O to an FEP Teflon pouch. Re_2O_7 is extremely hygroscopic, and was first weighed in an N_2-filled glovebox and immediately transferred to the Teflon pouch outside the glovebox. The pouch was heat sealed and placed inside a 125-mL Teflon-lined stainless steel reaction vessel which was backfilled with ~42 mL of deionized H_2O before closing. The reaction vessel was heated to 150 °C for 24 h inside a convection oven and slowly cooled to room temperature at 6 °C/h. Small red crystals of **I** were recovered without delay by filtration (0.159 g) in ~40% yield based on pzc. However, when the reaction products were allowed to age at room temperature after cooling for ~3 days inside the pouch, crystallization of the blue $[Cu(pzc)(H_2O)ReO_4]\cdot 2H_2O$ **II** solid (~0.33 g) occurred in ~100% yield, based on the remaining amount of pzc (after subtraction for the red solid). The red crystals of **I** were produced during the hydrothermal reaction, while the blue crystals of **II** subsequently crystallized at room temperature and pressure. Powder X-ray diffraction patterns revealed 100% of each respective product was the target compound, as judged from a comparison of the theoretical and experimental powder patterns.

X-ray Crystal Analysis. Both red and blue single crystals were selected for data collection at 100 K on a Bruker SMART APEX 4k CCD single-crystal diffractometer equipped with a normal-focus, 2.4-kW sealed-tube X-ray source (graphite monochromatized Mo Kα radiation, $\lambda = 0.71073$ Å) operating at 50 kV and 40 mA. The diffraction data were obtained by collection of 606 frames at each of three φ settings (0, 120, and 240°) using a scan width of 0.3° in ω and exposure times for the blue and red samples of 10 and 20 s/frame, respectively. At the end of the data collection, 50 initial frames were re-collected to monitor and correct for crystal decay.

Initial unit cell parameters for both samples were determined using Bruker's SMART program.[30] The parameters were then used to integrate all the respective data in Bruker's SAINT program,[30] where global refinement of the unit cell parameters was also performed to give the final values utilized in the subsequent structural refinements. Absorption corrections were applied using the empirical psi scan method via XPREP[31] for the blue sample, while for the red sample the data was processed through SADABS for correction of absorptions.[32] The structures were solved via direct methods using Bruker's SHELXS program,[31] and refined via full-matrix least squares against F^2 on all data using SHELXL.[31] Refinement of the electron density of the O5 position in **II** indicated disorder on this site, and it was modeled as a split position separated by ~1.0 Å. The O5 site faces toward a small channel window (see results section), which could account for the disorder. Positions for all non-hydrogen atoms were refined anisotropically for each structure, followed by a mixed independent refinement and

(11) Kim, D. S.; Wachs, I. E. *J. Catal.* **1993**, *141* (2), 419.
(12) Mandelli, D.; van Vliet, M. C. A.; Arnold, U.; Sheldon, R. A.; Schuchardt, U. *J. Mol. Catal. A* **2001**, *168*, 165.
(13) Moulijn, J. A. *J. Mol. Catal.* **1988**, *46* (1−3), 1.
(14) (a) Viswanadham, N.; Shido, T.; Iwasawa, Y. *J. Phys. Chem. B* **2002**, *106* (42), 10955. (b) Viswanadham, N.; Shido, T.; Sasaki, T.; Iwasawa, Y. *Stud. Surf. Sci. Catal.* **2003**, *145* (Science and Technology in Catalysis 2002), 189.
(15) Yuan, Y.; Iwasawa, Y. *J. Phys. Chem. B* **2002**, *106* (17), 4441.
(16) Szabo, S.; Bakos, I. *Stud. Surf. Sci. Catal.* **1998**, *118* (Preparation of Catalysts VII), 269.
(17) Jones, G. A.; France, C. A.; Ravinder, D.; Blythe, H. J.; Fedosyuk, V. M. *J. Magn. Mater.* **1998**, *184*, 28.
(18) Mendez, E.; Cerda, M. F.; Castro Luna, A. M.; Zinola, C. F.; Kremer, C.; Martins, M. E. *J. Coll. Interface Sci.* **2003**, *263* (1), 119.
(19) Schrebler, R.; Merino, M.; Cury, P.; Romo, M.; Cordova, R.; Gomez, H.; Dalchiele, E. A. *Thin Solid Films* **2001**, *388*, 201.
(20) Petrova, R.; Angelova, O.; Macicek, J. *Acta Crystallogr. C* **1996**, *52*, 1935.
(21) Macicek, J.; Angelova, O.; Petrova, R. *Z. Kristallogr.* **1995**, *210*, 24.
(22) Macicek, J.; Angelova, O.; Petrova, R. *Z. Kristallogr.* **1995**, *210*, 319.
(23) Macicek, J.; Angelova, O. *Acta Crystallogr. C* **1995**, *51*, 2539.
(24) Angelova, O.; Macicek, J.; Petrova, R.; Todorov, T.; Mihailova, B. *Z. Kristallogr.* **1996**, *211*, 163.
(25) Zhao, J.; Wang, J.; Zang, S.; Liu, S.; Yinling, S. *Rare Met.* **2001**, *20*, 28.
(26) Chakravorti, M. C.; Sarkar, M. B. *J. Ind. Chem. Soc.* **1983**, *60*, 628.
(27) (a) Gardberg, A. S.; Doan, P. E.; Hoffman, B. M.; Ibers, J. A. *Angew. Chem., Int. Ed.* **2001**, *40*, 244. (b) Gardberg, A. S.; Deng, K.; Ellis, D. E.; Ibers, J. A. *J. Am. Chem. Soc.* **2002**, *124*, 5476.
(28) Gardberg, A. S.; Sprauve, A. E.; Ibers, J. A. *Inorg. Chim. Acta* **2002**, *328*, 179.
(29) Sharma, C. V. K.; Griffin, S. T.; Rogers, R. D. *Chem. Commun.* **1998**, 215.
(30) *SMART Ver. 5.625 Data Collection and SAINT-Plus Ver. 6.22 Data Processing for SMART System*; Bruker Analytical X-ray Instruments, Inc.:, Madison, WI, 2001.
(31) Sheldrick, G. M. *SHELXTL NT ver. 6.10, Software Package for the Refinement of Crystal Structures*; Bruker Analytical X-ray Instruments, Inc.: Madison, WI, 2000.
(32) Sheldrick, G. M. *SADABS ver. 2.03, Software for Area Detector Absorptions and Other Corrections*; Bruker Analytical X-ray Instruments, Inc.: Madison, WI, 2001.

Table 1. Selected Crystal and Refinement Data for **I** and **II**

compound	**I** $[Cu_2(pzc)_2(H_2O)_2ReO_4]$	**II** $[Cu(pzc)(H_2O)ReO_4]\cdot 2H_2O$
fw	659.50	454.85
space group, Z	*Pnma* (No. 62), 4	$P2_1/n$ (No. 14), 4
T (K)	100(2)	100(2)
a, Å	7.4949(9)	8.5878(9)
b, Å	24.975(3)	12.920(1)
c, Å	9.141(1)	9.741(1)
β (deg)	90	92.830(2)
V	1711.1(4)	1079.4(2)
μ (Mo Kα), mm^{-1}	9.581	13.195
d_{calc}, g cm^{-3}	2.56	2.80
number of reflns	17064	11210
data/restraints/params	2167/0/141	2674/0/171
final $R1[I > 2\sigma(I)]$, $wR2^a$	0.026, 0.059	0.020, 0.053

^{a} $R1 = \sum||F_o| - |F_c||/\sum|F_o|$; $wR2 = \{\sum[w(F_o^2 - F_c^2)^2]/\sum[w(F_o^2)^2]\}^{1/2}$, $w = \sigma_F^{-2}$.

Table 2. Selected Atomic Coordinates and Equivalent Isotropic Displacement Parameters (Å^2 × 10^3) for $[Cu_2(pzc)_2(H_2O)_2ReO_4]$ (**I**)

atom^a	Wyckoff letter	x	y	z	U(eq)^b
Re	4c	0.19940(3)	0.25	−0.00029(2)	0.01941(8)
Cu1	4a	0	0.5	0	0.0105(1)
Cu2	4c	0.68359(8)	0.25	0.08408(7)	0.0114(1)
O1	8d	0.2679(4)	0.4617(1)	−0.0797(3)	0.0146(5)
O2	8d	0.9958(3)	0.4182(1)	0.3723(2)	0.0128(5)
O3	4c	0.4256(6)	0.25	−0.0017(5)	0.053(2)
O4	4c	0.1179(5)	0.25	0.1772(4)	0.0204(8)
O5a^c	8d	0.164(1)	0.3188(4)	−0.0625(9)	0.049(2)
O5b^c	8d	0.091(1)	0.2880(3)	−0.1155(8)	0.049(2)
O6	8d	0.0527(3)	0.4812(1)	0.2044(2)	0.0131(5)
N1	8d	0.8873(4)	0.4261(1)	−0.0028(3)	0.0098(5)
N2	8d	0.7601(4)	0.3233(1)	0.0501(3)	0.0115(6)
C1	8d	0.9913(4)	0.4359(1)	0.2465(4)	0.0100(6)
C2	8d	0.9048(4)	0.4025(1)	0.1290(4)	0.0098(6)
C3	8d	0.8436(4)	0.3514(1)	0.1549(4)	0.0112(7)
C4	8d	0.7383(5)	0.3475(1)	−0.0801(4)	0.0132(7)
C5	8d	0.8017(5)	0.3987(1)	−0.1065(4)	0.0141(7)

^{a} Hydrogen atoms, not listed, were constrained to ride on the parent carbon and oxygen atoms in idealized positions. ^{b} U(eq) is defined as one-third of the trace of the orthogonalized U_{ij} tensor. ^{c} The occupancies of O5a and O5b were refined as 0.5 each, a split position.

Table 3. Selected Atomic Coordinates and Equivalent Isotropic Displacement Parameters (Å^2 × 10^3) for $[Cu(pzc)(H_2O)ReO_4]\cdot 2H_2O$ (**II**)

atom^a	Wyckoff letter	x	y	z	U(eq)^b
Re	4e	0.01413(1)	0.62428(1)	0.87080(1)	0.01016(7)
Cu	4e	−0.33801(5)	0.70814(3)	0.68271(4)	0.00953(1)
O1	4e	0.0084(3)	0.6967(2)	0.0206(2)	0.0159(5)
O2	4e	0.1213(3)	0.5132(2)	0.8986(3)	0.0184(5)
O3	4e	0.1055(3)	0.6969(2)	0.7489(3)	0.0157(5)
O4	4e	−0.1737(3)	0.5951(2)	0.8084(3)	0.0158(5)
O5	4e	−0.2212(3)	0.8305(2)	0.7492(2)	0.0132(5)
O6	4e	−0.0348(3)	0.9418(2)	0.6887(3)	0.0155(5)
O7	4e	−0.4405(3)	0.5828(2)	0.6133(3)	0.0114(4)
O8	4e	−0.7401(3)	0.5997(2)	0.5275(3)	0.0159(5)
N1	4e	−0.1865(3)	0.7138(2)	0.5332(3)	0.0106(5)
N2	4e	−0.4884(3)	0.7350(2)	0.8296(3)	0.0108(5)
C1	4e	−0.1177(4)	0.8650(2)	0.6697(4)	0.0110(6)
C2	4e	−0.0999(4)	0.8006(2)	0.5418(3)	0.0106(6)
C3	4e	−0.1749(4)	0.6519(3)	0.4244(3)	0.0118(6)
C4	4e	−0.0743(4)	0.6779(2)	0.3210(3)	0.0119(6)
C5	4e	−0.5005(4)	0.6729(2)	0.9393(3)	0.0112(6)

^{a} Hydrogen atoms were constrained to ride on the parent carbon and oxygen atoms in idealized positions. ^{b} U(eq) is defined as one-third of the trace of the orthogonalized U_{ij} tensor.

Table 4. Selected Interatomic Distances (Å) and Angles (deg) in $[Cu_2(pzc)_2(H_2O)_2ReO_4]$ (**I**)

atom 1	atom 2	mult.	distance	intra-polyhedral angles	
Re	O3		1.695(5)	O5b−Re1−O3	119.5(3)
	O4		1.733(4)	O5b−Re1−O4	115.3(3)
	O5a^a	2×	1.830(8)	O3−Re1−O4	111.1(2)
	O5b^a	2×	1.634(7)	O3−Re1−O5a	98.3(3)
				O4−Re1−O5a	103.9(3)
Cu1	O1	2×	2.340(3)	O6−Cu1−O6	180.0(1)
	O6	2×	1.967(2)	O6−Cu1−O1	88.6(6)
	N1	2×	2.029(3)	O6−Cu1−O1	91.5(1)
				O1−Cu1−O1	180.0
Cu2	O3		2.086(5)	O6−Cu1−N1	83.0(1)
	O4		2.237(4)	O6−Cu1−N1	97.0(1)
	N2	2×	1.942(3)	O1−Cu1−N1	88.9(1)
				N1−Cu1−N1	91.1(1)
H (H-bonds)	O6		2.01(5)	N2−Cu2−N2	140.8(2)
	O2		1.99(5)	N2−Cu2−O3	102.3(1)
				N2−Cu2−O4	102.8(9)
				O3−Cu2−O4	99.3(2)

^{a} The occupancies of O5a and O5b are 0.5 each.

constrained assignment of the hydrogen positions. Hydrogen atoms were constrained to ride on idealized positions around the 2-pyrazinecarboxylate rings. Final anisotropic refinement converged at $R1/wR2 = 2.6/5.9\%$ and $2.0/5.3\%$ and data-to-variable ratios of 15.4 and 15.6 for $[Cu_2(pzc)_2(H_2O)_2ReO_4]$ (**I**, red) and $[Cu(pzc)(H_2O)ReO_4]\cdot 2H_2O$ (**II**, blue), respectively. Some data collection and refinement parameters, as well as selected atomic coordinates and isotropic-equivalent displacement parameters, are listed in Tables 1, 2, and 3. Interatomic contacts for selected bonds within each structure are given in Tables 4 and 5. Included in the Supporting Information is a complete list of data collection, refinement, and anisotropic displacement parameters and all near-neighbor interatomic distances.

Spectroscopic and Thermogravimetric Analysis. Mid-infrared (400−4000 cm^{-1}) spectra were collected on pure samples of **I** and **II** using a Mattson Genesis II FTIR spectrometer operating at a resolution of 2 cm^{-1}. Both samples were ground and pelletized with dried KBr, transferred to the FTIR, and evacuated for 2−5 min before spectra acquisition. The thermogravimetric analyses were performed on a TA Instruments TGA Q50. Crystalline samples of 19.916 g of **I** and 33.948 g of **II** were weighed, equilibrated at room temperature, and heated at a rate of 2 °C/min to 250 and 300 °C, respectively. The weight of each sample was measured as a function of temperature and converted to weight % of room temperature.

Results and Discussion

Structure Descriptions. The red crystals of the composition $[Cu_2(pzc)_2(H_2O)_2ReO_4]$ (**I**) are comprised of a 3D-connected organic/inorganic framework with two primary

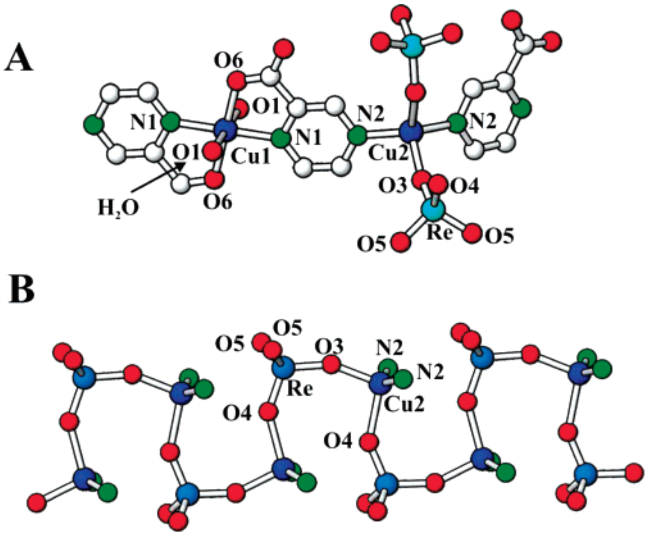

Figure 1. Two types of chains in $[Cu_2(pzc)_2(H_2O)_2ReO_4]$ (**I**), with atom types labeled. The mixed-valence copper chain, A, with Cu^{1+}/Cu^{2+} bonded through 2-pyrazinecarboxylate, and the alternating ReO_4/Cu^{1+} chain, B, bridging through oxygen.

Table 5. Selected Interatomic Distances (Å) and Angles (deg) in $[Cu(pzc)(H_2O)ReO_4]\cdot 2H_2O$ (**II**)

atom 1	atom 2	mult.	distance	intra-polyhedral angles	
Re	O1		1.736(2)	O2−Re−O3	107.6(1)
	O2		1.719(2)	O2−Re−O1	110.8(1)
	O3		1.732(2)	O3−Re−O1	108.5(1)
	O4		1.737(3)	O2−Re−O4	110.8(1)
				O3−Re−O4	108.8(1)
Cu1	O1		2.354(2)	O1−Re−O4	110.3(1)
	O4		2.335(3)	O7−Cu1−O5	176.2(1)
	O5		1.965(2)	O7−Cu1−N1	94.4(1)
	O7		1.948(2)	O5−Cu1−N1	82.6(1)
	N1		2.002(3)	O7−Cu1−N2	95.5(1)
	N2		2.005(3)	O5−Cu1−N2	87.8(1)
				N1−Cu1−N2	167.9(1)
H	O3		2.17(7)	O7−Cu1−O4	85.0(1)
(H-bonds)	O5		1.98(7)	O5−Cu1−O4	92.6(1)
	O6		1.85(7)	N1−Cu1−O4	90.4(1)
				N2−Cu1−O4	97.4(1)
				O7−Cu1−O1	88.4(1)
				O5−Cu1−O1	93.5(1)
				N1−Cu1−O1	81.7(1)
				N2−Cu1−O1	91.6(1)
				O4−Cu1−O1	169.32(9)

types of chains, illustrated in Figure 1. Each of the metal atom types and their local coordination environments are labeled, and the corresponding bond distances and angles can be found in Table 4. The upper chain, A, exhibits two different coordination environments for Cu, octahedral Cu1 and tetrahedral Cu2, that alternate down the chain and are bridged to each other through 2-pyrazinecarboxylate (2-pzc). Each Cu1 is equatorially chelated by the nitrogen and oxygen donor atoms of two pzc ligands (Cu1−O6 at 1.967(2) Å and Cu1−N1 at 2.029(3) Å) and is also bonded to two H_2O molecules (Cu1−O1 at 2.340(3) Å). Cu2 is also bridged to each pzc through the opposing (para) nitrogen group (Cu2−N2 at 1.942(3) Å), to form the backbone of the Cu(pzc) chain that runs down the *b*-axis in Figure 2, right (A). Cu2 is additionally bonded to two ReO_4 groups through oxygen (Cu2−O3, O4 at 2.086(5) and 2.237(4) Å, respectively), and forms the corrugated $Cu(pzc)ReO_4$ chain that runs down the *a*-axis, shown isolated in Figure 1B and within the network in Figure 2, left (B). Cu1 is bonded to two carboxylate groups, and is therefore formally +2 $[Cu^{2+}-(COO^-)_2]$, while each Cu2 is bonded to two bridging ReO_4^- groups and is formally +1 $[Cu^{1+}-(ReO_4^-)_{2/2}]$. The ReO_4 distances and angles span from 1.634(7) to 1.830(8) Å and 98 to 119.5°, similar to that in other perrhenate-containing solids.[20−29]

The overall 3D structure of **I** contains the two types of chains, Cu1(pzc)/Cu2(pzc) and $Cu2(pzc)/ReO_4$, oriented approximately perpendicular to each other and connected via the common Cu2 tetrahedra. Highly ellipsoidal channels are formed along *a*, with dimensions ∼3.3−4.7 Å × 12.5 Å, Figure 2, and are located roughly between neighboring $Cu2(pzc)/ReO_4$ chains. Dimensions of the closest interatomic contacts across the open space are marked. Two oxide groups (O5) of the perrhenate (ReO_4) are located along the walls, as are the carbon atoms of the pzc ligands. The ReO_4 groups are located in an accessible position within the channel to be a potentially catalytically active site for small molecules, likely as an oxidant.

The blue crystals of **II** are also comprised of intersecting $Cu(pzc)/ReO_4$ and Cu(pzc) chains that form a (4,4) square net, Figure 3. The symmetry-unique atoms and their local coordination environment are labeled in Figure 3A, and the associated interatomic distances and angles are given in Table 5. In contrast to the red solid, a single symmetry-unique Cu site is bonded to one carboxylate (−O5 at 1.965(2) Å) and to two bridging ReO_4^- groups (−O1 at 2.354(2) Å and −O4 at 2.335(3) Å), and is formally +2 $[Cu^{2+}-(COO^-)(ReO_4^-)_{2/2}]$. The local coordination environment of Cu is completed by one H_2O molecule (−O7 at 1.948(2) Å) and by N atoms of two pzc ligands (−N1 at 2.002(3) Å and −N2 at 2.005(3) Å). Each pzc ligand is chelating a single Cu in the square net, with another bond to Cu through the opposing N, arranged so that every carboxylate group points down roughly the [001] direction. However, in the next layer either above or below, shown in Figure 4, the carboxylate groups are oriented in the opposite direction, and results in the cancellation of any dipole moment, as required for the space group $P2_1/n$. The ReO_4 groups are similarly bridging, with a more uniform and narrower range of Re−O distances (1.719(2) − 1.737(3) Å) and angles (107.6 − 110.8°) than before.

The structure of **II** is also characterized by significant hydrogen bonding between many different chemical groups, drawn as dashed lines in Figures 3B and 4. Each open square within the polar net is ∼4.4 × 5.1 Å and is centered by a free H_2O molecule that hydrogen bonds (intralayer) to an oxide group on ReO_4 (O···H of 2.17(7) Å), to an oxide group of COO^- that is also bonded to Cu (O···H of 1.98(7) Å), and also to another coordinated H_2O molecule on Cu (O···H of 1.82(7) Å), Figure 3B. Removal of this guest H_2O molecule by heating, as verified later by TGA, would allow another small organic molecule to directly interact with the ReO_4 sites. In addition, there is substantial interlayer hydrogen bonding between the two sheets, Figure 4, which occurs between the Cu-coordinated H_2O molecules of one layer and the alcohol group (or free end) of the carboxylate

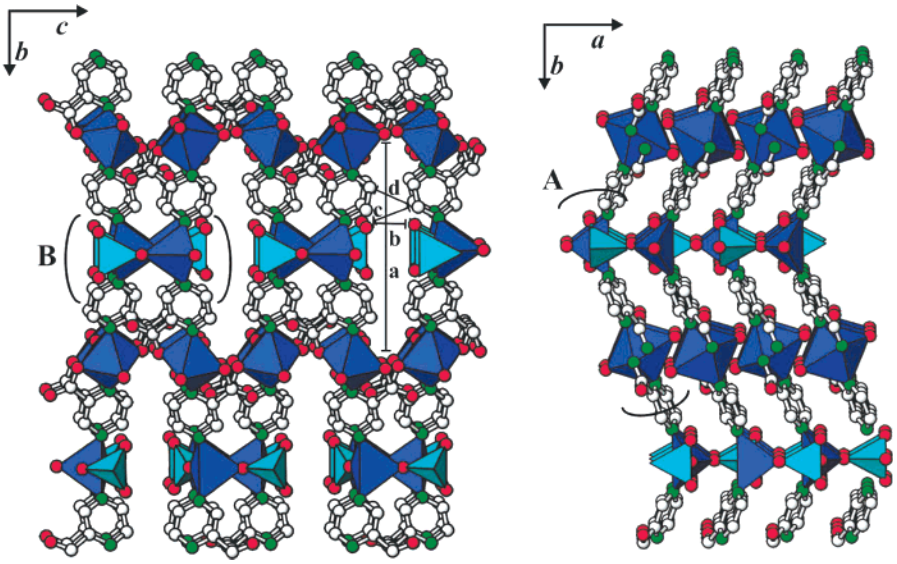

Figure 2. Views (~[100] and ~[001]) of the $[Cu_2(pzc)_2(H_2O)_2ReO_4]$ (**I**) structure, with polyhedral Re (light blue) and Cu (dark blue) coordination environments. The two types of chains drawn in Figure 1 are labeled A and B. The marked dimensions of the channel (left) are a = 12.5 Å, b = 4.7 Å, c = 3.3 Å, d = 4.5 Å.

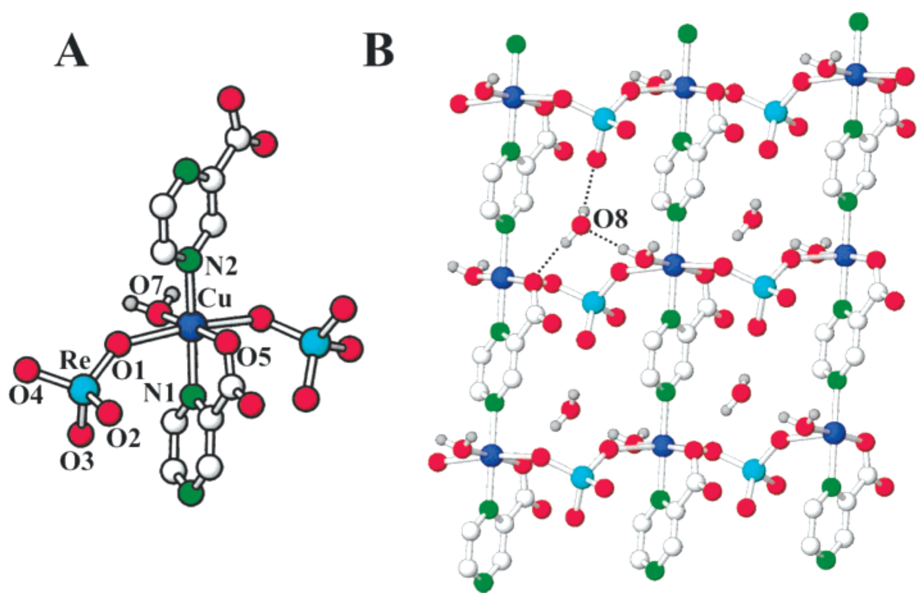

Figure 3. Left (A), the local environment of Cu^{2+} with atom types labeled, and right (B), the approximately square net (4,4) in $[Cu(pzc)(H_2O)ReO_4]\cdot 2H_2O$ (**II**). Hydrogen bonds to internal H_2O molecules are drawn as dashed lines in B.

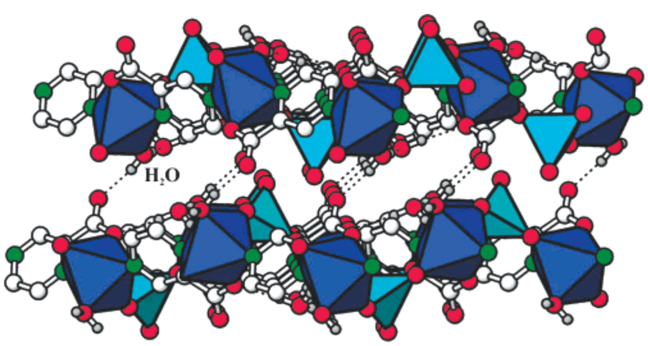

Figure 4. An ~[100] view of the layered structure of $[Cu(pzc)(H_2O)ReO_4]\cdot 2H_2O$ (**II**), with the interlayer hydrogen bonds drawn as dashes. Each layer is identical to that in Figure 3.

ligand of the neighboring layer (O···H of 1.85(7) Å). The substantially greater hydrogen bonding for **II** is expected both from the higher H_2O content as well as from its layered structure that crystallizes at room temperatures and pressures.

Infrared Spectroscopy and Thermogravimetric Analyses. The observed infrared absorption bands could be matched, using standard IR libraries and known compounds,[33−35] with the number of types of bonds and elements present in both structures. For $[Cu_2(pzc)_2(H_2O)_2ReO_4]$ (**I**), characteristic peaks are present for C=O stretches (1645 cm^{-1}), for Re−O stretches (862, 894 and 923 cm^{-1}),[35] and for many C−C and C−H vibrations. A broad but relatively small IR peak is observed at approximately 3448 cm^{-1} for

(33) Nakamoto, K. *Infrared and Raman Spectra of Inorganic and Coordination Compounds*, *Part A*; John Wiley & Sons: New York, 1997.
(34) Pouchert, C. J. *The Aldrich Library of FT-IR Spectra*; Aldrich Chemical Co.: Milwaukee, WI, 1997.
(35) John, G. H.; May, I.; Sarsfield, M. J.; Steele, H. M.; Collison, D.; Helliwell, M.; McKinney *Dalt. Trans.* **2004**, 734.

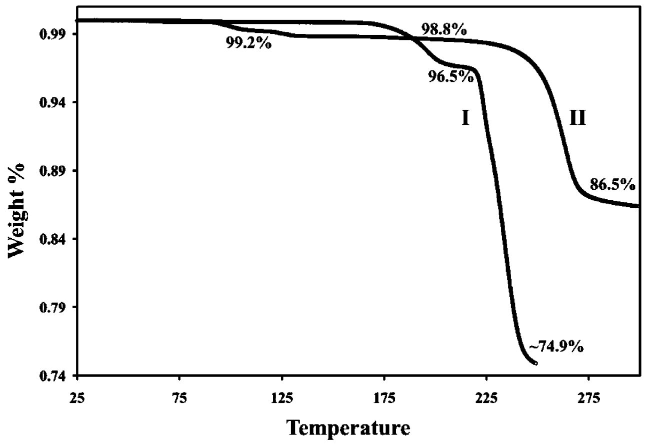

Figure 5. Thermogravimetric curves for solids **I** and **II**, with the value for each temperature calculated as the percent weight.

O−H groups in the structure, as expected for the relatively small amount of structural water. While for [Cu(pzc)(H_2O)-ReO_4]·2H_2O (**II**), characteristic peaks are present for C=O stretches (1657 and 1608 cm^{-1}), a very strong peak for the Re−O stretching vibration (908 cm^{-1}), and the same characteristic C−C and C−H stretches. A broad absorption peak characteristic for O−H groups is centered at approximately 3426 cm^{-1}, and is more intense than that in **I**, as expected for the higher amount of structural water. Absorption peaks for Cu−N and Cu−O bond vibrations were not located in the detectable range of frequencies.

The thermogravimetric analyses indicate that the H_2O content of both **I** and **II** is lost at elevated temperatures beginning at ∼180 °C and ∼225 °C, respectively, shown in Figure 5. [Cu_2(pzc)$_2$(H_2O)$_2$$ReO_4$] (**I**) is calculated to contain 5.46 wt % H_2O, while the sample loses up to 3.5 wt % before decomposition begins to occur at 225 °C and higher temperatures. This weight loss corresponds to only 64% of the H_2O content, which is, however, entirely coordinated to Cu in the structure. [Cu(pzc)(H_2O)ReO_4]·2H_2O (**II**), consists of 3.96 wt % of coordinated H_2O and 7.91 wt % of "free" (only hydrogen-bonded) H_2O within the stacked layers of square nets. TGA analysis of **II** revealed a relatively small loss of sample weight (1.2 wt %) at ∼100 °C (likely from the loss of adsorbed and/or intergrain H_2O), while beginning at 225 °C, a 12.3 wt % loss occurs. The latter weight loss compares relatively well with the combined H_2O content of **II** (11.9%), and indicates the total loss of structural H_2O at temperatures of 250→300 °C, and not a stepwise elimination of the coordinated and "free" H_2O molecules. Powder X-ray diffraction of **I** and **II** reveals both lose crystallinity at temperatures where maximum H_2O desorption occurs, and both eventually decompose into unidentified black solids. However, at up to ∼195−210 °C for **II**, the color of the solid changes to green and by X-ray powder diffraction appears to retain the same crystal structure, though poorly crystalline.

Conclusions

Research efforts to uncover potentially catalytically active open framework solids led us to the discovery of two new ReO_4-containing structures, [Cu_2(pzc)$_2$(H_2O)$_2$$ReO_4$] (**I**) and [Cu(pzc)($H_2O$)$ReO_4$]·2$H_2O$ (**II**). These solids feature some of the first examples of open framework structures containing the perrhenate anion (ReO_4^-), one (**I**) an extended 3D network with ellipsoidal channels, and another (**II**) a layered structure with "free" H_2O molecules within square nets. Both solids feature −Cu−O−Re−O− chains that are connected into a higher dimensional structure via 2-pyrazinecarboxylate ligands. TGA results reveal both solids exhibit either partial or total dehydration, which potentially allows small molecule access to ReO_4^- oxidation sites throughout the micropores of **I** or the open framework of **II**.

Acknowledgment. We thank Jaap Folmer for assistance with the thermogravimetric analysis. PM acknowledges support from NCSU for startup funds and TW acknowledges support from the National Science Foundation (NSF) CCLI Grant (0087210) and the Ohio Board of Regents Action Fund (CAP-491) for the purchase of the CCD X-ray diffractometer.

Supporting Information Available: Infrared and X-ray crystallographic files in CIF format, including tables of crystallographic details, atomic coordinates, anisotropic thermal parameters, and interatomic distances and angles; and absorption graphs (pdf). This material is available free of charge via the Internet at http://pubs.acs.org.

IC049609H